교란 유한요소법을 이용한 하드 디스크 슬라이더의 동특성 해석

황 평 [1](영남대학교 기계공학부), 콴 폴리나 [2](영남대학교 기계공학과)

Dynamic Characteristics of HDD Slider by Perturbed Finite Element Method

[1]Pyung Hwang (School of Mechanical Engineering, Yeungnam University) *phwang@yumail.ac.kr*,
[2]Polina V. Khan* (Mechanical Engineering Department, Yeungnam University) *polina@yumail.ac.kr*.

ABSTRACT

The numerical analysis of the hard disk drive slider is presented. The pressure distribution was calculated using the finite element method. The generalized Reynolds equation was applied in order to include the gas rarefaction effect. The balance of the air bearing force and preload force was considered. The characteristics of the small vibrations near the equilibrium were studied using the perturbation method. Triangular mesh with variable element size was employed to model the two-rail slider. The flying height, pitching angle, rolling angle, stiffness and damping of the two-rail slider were calculated for radial position changing from the inner radius to the outer radius and for a wide range of the slider crown values. It was found that the flying height, pitching angle and rolling angle were increased with radial position while the stiffness and damping coefficients were decreased. The higher values of crown resulted in increased flying height, pitching angle and damping and decreased stiffness.

Keywords : FEM, HDD slider, perturbation.

Nomenclature

C = damping coefficient
D = Knudsen number
G = perturbed pressure
H = dimensionless film thickness
h = film thickness
h_f = flying height
j = imaginary unit
K = stiffness coefficient
L = total vertical force
M = moments
P = dimensionless pressure
p = pressure
Q = flow rate coefficient
s = film thickness variation
T = dimensionless time
U,V = dimensionless velocity
W = preload
X, Y = dimensionless coordinates
ϕ = pitching angle
Λ = compressibility number
σ = squeeze number
θ = rolling angle

1. Introduction

The main computer data storage, such as the hard disk drive (HDD) has several heads (sliders) and disks. The elements that read and write the magnetic records on the disk are mounted on the heads. *The main requirements for modern HDDs* are high data storage density and reliability. This means that the slider must have low flying height, fast take-off, and high resistance to external excitations. So new slider designs are developed and analyzed to satisfy these requirements.

During the disk rotation high pressure is generated in the air film between the slider and disk's surfaces. The resultant of the air bearing

force and suspension force acts on the slider and defines its flying attitude.

The distribution of pressure in the air film is described by the nonlinear Reynolds equation, which can be solved using the finite difference method [1], finite element method [2-4] or finite volume method [5]. Variable mesh spacing is essential for slider analysis in the high compressibility number region to resolve the boundary layer. The FDM and direct numerical method [6] utilize the transformed grid. The FEM and FVM can be used with unstructured meshes [7].

When the flying height becomes smaller than the air molecular mean free path, the Boltzmann equation solution is required for correct representation of the boundary conditions. Fukui and Kaneko [8] proposed the database of the flow rate coefficients obtained by the numerical solution of the Boltzmann equation.

Full dynamic simulation can be very time consuming process. The basic information about dynamic behavior of the slider can be obtained by using the linearized approach. First the static Reynolds equation must be solved together with the equilibrium equations [2, 4, 9-14]. After this, the perturbation method is applied to evaluate stiffness and damping coefficients in vicinity of the steady state position [2, 13, 14].

2. Numerical procedures

2.1 Fundamental equations

The steady state distribution of pressure in the air film between the slider and the disk is described by the nonlinear generalized Reynolds equation, which can be written in dimensionless form as:

$$\frac{\partial}{\partial X}\left(Q(D)H^2\frac{\partial P}{\partial X}\right)+\frac{\partial}{\partial Y}\left(Q(D)H^2\frac{\partial P}{\partial Y}\right) = \Lambda\left(\frac{\partial(UPH)}{\partial X}+\frac{\partial(VPH)}{\partial Y}\right)+\sigma\frac{\partial(PH)}{\partial T} \quad (1)$$

where $H(X, Y)$ is the dimensionless air film thickness, $P(X, Y)$ is the dimensionless pressure, $U(X, Y)$ and $V(X, Y)$ are the dimensionless disk surface velocity components, Λ is the compressibility number:

$$\Lambda=\frac{6u_0\mu l}{p_a h_o^2}=\frac{6r_0\omega\mu l}{p_a h_o^2} \quad (2)$$

D is the inverse Knudsen number, $D=D_0PH$, and

$$Q(D)=PHQ_p/Q_c=6Q_p/D_0 \quad (3)$$

is the flow rate coefficient. Continuum flow rate is $Q_c=D/6$. $Q_P(D)$ is obtained from the flow rate database proposed by Fukui and Kaneko [6], using the local interpolation method.

The Reynolds equation is solved using Bubnov-Galerkin finite element method with triangular mesh elements [2, 15].

2.2 Static analysis

The attitude of the slider is described by the vector, consisting of the flying height, h_f, the pitching angle, ϕ, and the rolling angle, θ(Fig. 1). The film thickness distribution depends on the

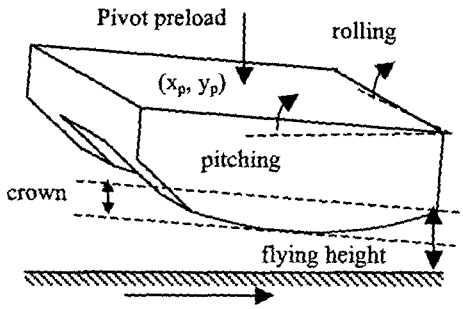

Fig. 1 Slider parameters and coordinates

slider's shape and attitude:

$$h(x,y) = h_s(x,y) + h_f + \phi(x_r - x) + \theta(y_r - y) \quad (4)$$

where $h_S(x, y)$ is the function of slider surface shape, and (x_r, y_r) is the rotation center.

For the given shape of the slider and fixed disk surface velocity field, the distribution of the pressure in the air film is the function of the slider's attitude.

The total vertical force and the pitching and rolling moments include the air bearing force terms and pivot preload terms:

$$\begin{aligned} L(h_f,\phi,\theta) &= -W + \int p dxdy \\ M_\phi(h_f,\phi,\theta) &= W(x_p - x_b) - \int p(x - x_b)dxdy \\ M_\theta(h_f,\phi,\theta) &= W(y_p - y_b) - \int p(y - y_b)dxdy \end{aligned} \quad (5)$$

where (x_p, x_p) is the preload application point and (x_b, x_b) is the balancing center. When the slider is at the steady state attitude, the objective vector is equal to zero.

$$(L, M_\phi, M_\theta) = (0,0,0) \quad (6)$$

In the present work the system (6) is solved iteratively using the conjugate-gradient method [11, 12, 16].

2.3 Dynamic coefficients

Consider the small harmonic deviation of the film thickness and pressure from the steady state values $\bar{h}$ and $\bar{p}$:

$$\begin{aligned} h &= \bar{h} + \varepsilon \hat{h} e^{j\nu} \\ p &= \bar{p} + \varepsilon \hat{p} e^{j\nu} \end{aligned} \quad (7)$$

When substituted to equation (1) it gives the linearized Reynolds equation that can be solved with respect to pressure variation $\hat{p}$.

The film thickness perturbation is a combination of small displacements in vertical, pitching and rolling directions

$$\hat{h}(x,y) = \hat{h}_f + \hat{\phi}(x - x_c) + \hat{\theta}(y - y_c) \quad (8)$$

The perturbed pressure corresponding to unit displacements is denoted by G_i - complex stiffness

$$\hat{p} = G_1\hat{h}_f + G_2\hat{\phi} + G_3\hat{\theta} = \sum G_i \hat{s}_i \quad (9)$$

The air film stiffness and damping matrixes are expressed as follows [2, 12]

$$\begin{aligned} K_{1,j} &= \frac{\partial L}{\partial s_j} = \iint \Re(G_j) dxdy \\ K_{2,j} &= \frac{\partial M_\phi}{\partial s_j} = \iint \Re(G_j)(x - x_c) dxdy \\ K_{3,j} &= \frac{\partial M_\theta}{\partial s_j} = \iint \Re(G_j)(y - y_c) dxdy \end{aligned} \quad (10)$$

$$\begin{aligned} C_{1,j} &= \frac{\partial L}{\partial \dot{s}_j} = \frac{1}{j\nu} \iint \Im(G_j) dxdy \\ C_{2,j} &= \frac{\partial M_\phi}{\partial \dot{s}_j} = \frac{1}{j\nu} \iint \Im(G_j)(x - x_c) dxdy \\ C_{3,j} &= \frac{\partial M_\theta}{\partial \dot{s}_j} = \frac{1}{j\nu} \iint \Im(G_j)(y - y_c) dxdy \end{aligned} \quad (11)$$

3. Computation results

3.1 Two-rail slider

The two-rail slider (Fig. 1) is one widely used in commercial Hard Disk Drivers, such as the IBM 3370 and IBM 3380. In the present work, the so called 50% slider, with 2 mm length and 1.6 mm width is considered to provide the flying height at about 50 nm, which is usual for modern HDD. The rail width is 0.154 mm, the front taper length is 0.2 mm and the taper angle is 10 mrad. The pivoting preload of 0.0343 N is applied at the slider's center.

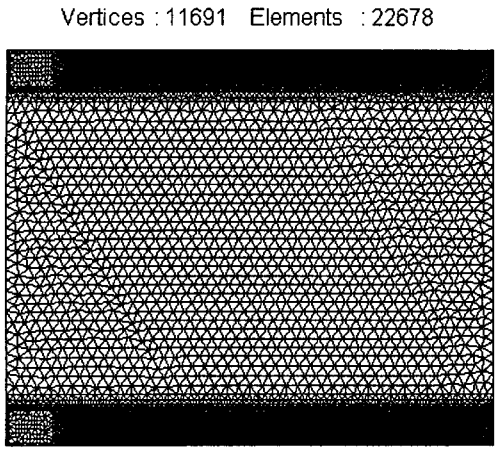

Fig. 2. The unstructured triangular mesh for slider analysis

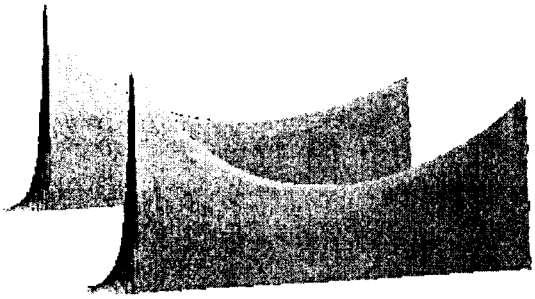

Fig. 3. The distribution of pressure at the steady state for 15 nm crown, 15 mm radial position

The mesh (Fig. 2) is refined at the trailing edge where the pressure distribution has steep gradient. The small elements are used along the whole rails, so that the "ridges" in pressure distribution (Fig. 3) can be smoothly interpolated.

3.2 Static characteristics

The steady state attitude of the slider is shown in Fig. 4-6 for the two-rail sliders with different crown values. The flying height is increased with radial position almost two times. The pitching angle and rolling angle are also increased.

The increase of the crown results in uniform increases in the flying height (Fig. 4) and pitching angle (Fig. 5) for the whole range of the slider's radial position, from the inner to the outer radius of the disk. The rolling angle (Fig. 6) decreases with increasing crown at the inner radius and increases at the outer radius.

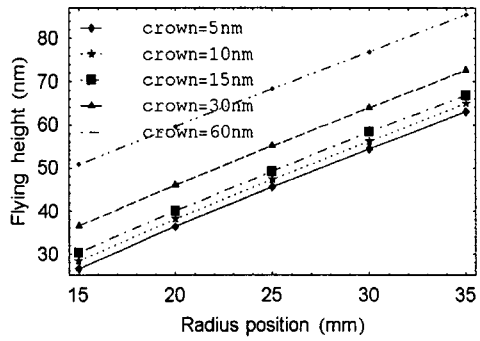

Fig. 4 The flying height at the steady state

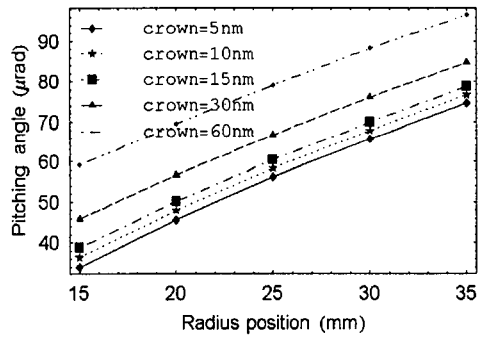

Fig. 5 The pitching angle at the steady state

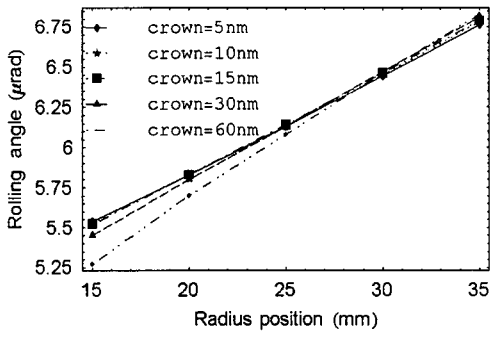

Fig. 6 The rolling angle at the steady state

3.3 Dynamic characteristics

Figures 7,8 show the air bearing stiffness and damping coefficients for vertical oscillations. The stiffness is decreased with radial position from 1.1MN/m at the inner radius to 0.5MN/m at the outer radius. The highest stiffness corresponds to the smallest crown values (Fig. 7). The damping is also decreased with radius from 4N*s/m at the inner radius to 1N*s/m at the outer radius. In contrast with the stiffness, the damping is increased with crown (Fig. 8).

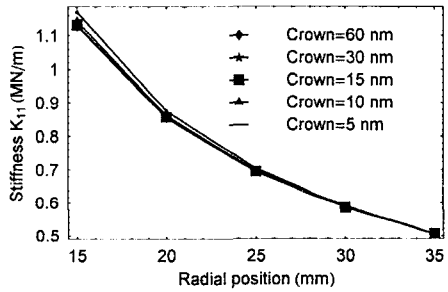

Fig. 7 Stiffness for vertical oscillations

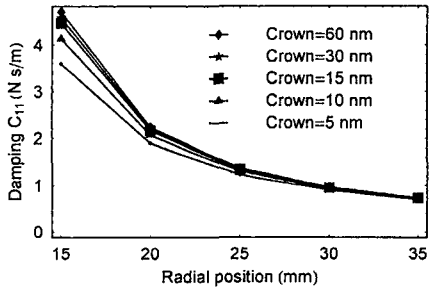

Fig. 8 Damping for vertical oscillations

4. Conclusions

The small vertical oscillations of the two-rail slider were studied by using the perturbed FE analysis. The stiffness and damping coefficients were considered as functions of the radial position and crown.

The stiffness was decreased with both radial position and crown as a result of increased flying height.

The damping was also decreased with radial position but it was increased with crown.

References

1. White, J. W, "Flying Characteristics of the Transverse and Negative Pressure Contour (TNP) Slider Air Bearing," ASME J. of Tribology, Vol. 119, pp. 241-248, 1997.
2. Mitsuya, Y., and Ota, H., "Stiffness and Damping of Compressible Lubrication Films Between Computer Flying heads and Textures Media: Perturbation Analysis Using Finite Element Method," ASME J. of Tribology, Vol. 113, pp. 819-827, 1991.
3. Faria, M.T.C., and Andres, L.S., "On the Numerical Modeling of High-Speed Hydrodynamic Gas Bearings," ASME J. of Tribology, Vol. 122, pp. 124-130, 2000.
4. Peng, J. P., and Hardie, C. E., "Characteristics of the Air Bearing Suction Force in Magnetic Recording Disks," ASME J. of Tribology, Vol. 118, pp. 549-553, 1996.
5. Zeng, Q. H., and Bogy, D. B., "Stiffness and Damping Evaluation of Air Bearing Slider and New Designs With High Damping," ASME J. of Tribology, Vol. 121, pp. 341-347, 1999.
6. Kawabata, N., "A Useful Numerical Analysis Method for the Dynamic Characteristics of Fluid Film Lubrication (The case of Incompressible Fluid

Lubrication)," JSME Int. J., Vol. 34, No. 1, pp. 91-96, 1991.

7. Wu, L., and Bogy, D. B., "Unstructured Adaptive Triangular Mesh Generation Techniques and Finite Volume Schemes for the Air Bearing Problem in the Hard Disk," ASME J. of Tribology, Vol. 122, pp. 761-770, 2000.
8. Fukui, S., and Kaneko, R., "A Database for the Interpolation of Poiseuille Flow Rate for the High Knudsen Number Lubrication Problems," ASME J. of Tribology, Vol. 112, pp. 78-83, 1990.
9. Choi, D.-H., and Yoon S.-J., "Static Analysis of Flying Characteristics of the Head Slider by Using an Optimization Technique," Transactions of the ASME, Vol. 116, pp. 90-94, 1994.
10. Hwang, P., Park, S. S., and Kim, E., "A Study on Lubricative Characteristics of the Negative Pressure Slider," KSTLE Int. J, Vol. 3, No. 2, pp. 110-113, 2002.
11. Khan, P. V., and Hwang, P, "On Application of the Conjugate-Gradient Method to Static Analysis of HDD Slider," Proc. 38th spring conference of KSTLE, 2004.
12. Hwang, P., Khan, P., and Kim, E.-H., "Finite Element Analysis Of Computer Hard Disk Drive Slider Using Optimization Scheme," Proc. Joint Symposium between Sister Universities in Mechanical Engineering (JSSUME), Yokogama, pp. 239-244, 2004.
13. Ono, K., "Dynamic Characteristics of Air-Lubricated Slider Bearing for Noncontact Magnetic Recording," ASME J. of Lubrication Technology, Vol. 97, pp. 250-260, 1975.
14. Khan, P. V., and Hwang, P., "Dynamic Characteristics of HDD Slider by Perturbated Direct Numerical Method," Proc. 37th autumn conference of KSTLE, 2003.
15. Huebner, K. H., Thornton, E. A., and Byrom, T. G., "*The Finite Element Method for Engineers,*" John Wiley & Sons, New York, pp. 137-141, 1995.
16. Bazaraa, M. S., and Shetty, C. M., "*Nonlinear programming,*" John Wiley & Sons, New York, pp. 289-316, 1979.